Applied Chemistry Today **19(73)** (2024) 11-26

Semnan University

Applied Chemistry Today

Journal homepage: https://chemistry.semnan.ac.ir/

ISSN: 2981-2437

Research Article

Electrochemical Characteristics and Supercapacitance of the Self-Assembled Catocene Complex on Carbon Microfiber Electrode

Sajjad Damiri*, Zahra Samiei, Hamid Reza Pouretedal

Department of Applied Chemistry, Maleke-ashtar University of Technology, Shahin-shahr, Esfahan, I. R. Iran

PAPER INFO

Article history:
Received: 31/Jan/2024
Revised: 11/Apr/2024
Accepted: 15/Apr/2024

Keywords:
Supercapacitor,
Catocene,
Carbon microfiber,
Electrochemical,
Specific capacity.

ABSTRACT

To prevent a potential energy crisis in the near future, it is necessary to develop high-performance energy storage devices, such as supercapacitors (SCs). In this study, we fabricated a thin film of a new redox catalyst, catocene, on a carbon microfiber electrode (Cat/CMF) using a self-assembled method. We then investigated its electrochemical behaviour in an aqueous sodium sulfate electrolyte. Different techniques were used to evaluate the surface quality of the thin film and its iron content, including scanning electron microscopy (SEM), laser-induced breakdown spectroscopy (LIBS), and attenuated total reflection infrared spectroscopy (ATR). The efficiency and specific capacity of the electrodes were then assessed using cyclic voltammetry (CV), electrochemical impedance spectroscopy (EIS), and galvanostatic charge-discharge (GCD) methods in a three-electrode system. Electrochemical tests revealed that the redox processes are diffusion-controlled, exhibiting battery-like behaviour. The cathodic transfer coefficient is close to 0.48, and the charge transfer resistance of the modified electrode is improved up to 23 times compared to the bare electrode. At a current density of 0.55 A/g, the specific capacity of the Cat/CMF electrode is 39.76 F/g. At a current density of 0.83 A/g, the catocene thin film exhibits a supercapacitance behaviour with an energy density of 2.5 Wh/kg and a power density of 373.8 W/kg.

DOI: https://doi.org/10.22075/chem.2024.33122.2250

* **Corresponding author:** Associate Professor of Analytical Chemistry. *E-mail address: s_damiri@mut-es.ac.ir*

How to cite this article: Damiri, S., Samiei, Z., & Pouretedal, H. R. (2024). Electrochemical Characteristics and Supercapacitance of the Self-Assembled Catocene Complex on Carbon Microfiber Electrode. *Applied Chemistry Today*, **19(73)**, 11-26. (in Persian)

1. Introduction

Today, the demand for clean, lightweight, high-capacity, and cyclically stable electrical energy storage sources has increased due to the development of new technologies and environmental concerns. Research and development on electrochemical supercapacitors (SC) has received special attention due to their high power density, long cycle life (more than 100,000 cycles), and high charge-discharge rate compared to batteries and fuel cells [1,2]. There are two primary classifications of supercapacitors based on their energy storage mechanism: electrochemical double-layer capacitors (EDLC) and pseudo-capacitors. EDLCs accumulate electric charge at the electrode-electrolyte interface, while pseudo-capacitors store charge through reversible redox reactions on electrochemically active sites [3]. The challenge remains to design or use new, affordable, environmentally friendly, and efficient electrode active materials for effective electrical energy storage. In the past decade, various electrode active materials have been identified, including conductive polymers [4,5], transition metal oxides [6,7], metal complexes, and metal-organic frameworks [8,9] due to their relatively favourable electrochemical behaviour and charge storage capacity. To enhance the specific capacity of a capacitor and improve its electrical charge-discharge kinetics, various composites containing reactants and carbon materials such as graphite, graphene, carbon nanotubes, and carbon nanofibers [1,10] or porous metal microstructures [11,12] have been developed. These composites lighten and improve the microscopic surface area and electrical conductivity of electrodes.

The electrode is a crucial component of a supercapacitor, and its overall performance is greatly influenced by the design of its structure. Thin-film electrodes (TFEs) have been identified as an efficient domain in SC electrodes, with layer thickness ranging from several nanometers to several hundreds of micro-metres. In thin films, ion transfer and the rate of charge-discharge processes, which are among the main requirements of SCs, are accelerated, and the equivalent series resistance (ESR) is reduced. The active material's low loading weight on the electrodes slightly reduces the overall specific capacity. However, TFEs can be used in portable and miniaturized equipment [13,14].

It is valuable to implement TFEs on various carbon electrodes with a highly effective surface, such as Carbon Felts (CF). Various scientific research has been reported in the field of CF electrodes modified with various redox materials. For instance, V_2O_5 nanosheets assembled on carbon fibre felt as a free-standing electrode for flexible asymmetric supercapacitors exhibit specific capacity of 1465 mF cm^{-2} (492 $F.g^{-1}$), power density of 17.5 $mW.cm^{-3}$ at the energy density 0.928 $mWh.cm^{-3}$ [15]. The use of Binder-Free Electro-Deposited MnO_2 @3D Carbon Felt Network results in a maximum capacitance of 187.5 $F.g^{-1}$ at 0.2 $A.g^{-1}$ with a high-voltage window of 2 V [16]. Meanwhile, the application of Nickel ferrite ($NiFe_2O_4$) coated on a CF electrode demonstrates an energy density and power density of 39 Wh/kg and 410 W/kg [17]. The electrochemical performance of hydrothermal deposited urchin-like $NiCo_2O_4$ on carbon felt was found to have a high specific capacity of 243.1 $mAh.g^{-1}$ (0.278 $mAh.cm^{-2}$) at a current value of 2.0 mA and a capacity retention of approximately 91.3% after 5000 cycles in a 6 M KOH aqueous electrolyte [18]. Meanwhile, the self-supporting $CoSe_2$/carbon fibre felt electrode synthesized via microwave exhibited superior electrochemical performance, with a capacity of 621 $F.g^{-1}$ at 1.0 $A.g^{-1}$ and an energy density of 22.43 $Wh.Kg^{-1}$ at a power density of 823.12 $W.kg^{-1}$ [19].

In the development of TFEs or composite electrode active materials for fast charge-discharge supercapacitors, the chemical derivatization of redox materials such as ferrocene derivatives onto conductive porous electrodes is most commonly used, and this type of synthesis process is very expensive, and the amount of surface coverage of the grafted material is also relatively low [20–22]. For example, by using multi-walled carbon nanotubes (MWCNTs) functionalized with ferrocene complex, a specific capacitance of 50 $F.g^{-1}$ at a current density of 0.25 $A.g^{-1}$ with high cycling stability has been achieved [20]. Ferrocene-based polymer coordination has also been considered due to its high thermal stability, two stable redox states, fast electron transfer and excellent charge-discharge efficiency [21].

Solid active materials usually crystallize in surface adsorption methods, and their electrochemical efficiency decreases [23–26]. The use of liquid redox materials compared to solid ones, due to the ability of molecular absorption instead of crystalline particles, offers the possibility of more favourable interaction with carbon electrodes [27–29]. In this research, an attempt was made to analyze the electrochemical behaviour and energy storage of 2, 2′-bis(ethylferrocenyl) propane (catocene) complex as a liquid redox on the carbon microfiber (CMF) electrode with self-assembled layers and surface absorption fabrication method. Catocene is a dark brown-orange liquid with chemical formula $C_{17}H_{22}Fe$ and atomic mass 282.2 g/mol, which is used as an effective burn rate catalyst in solid propellants containing ammonium perchlorate [30–32].

2. Materials and Methods

2.1. Chemicals and Apparatus

All chemicals, such as sodium sulfate and dimethylformamide (DMF) solvent with analytical purity, were purchased from Merck Company. Carbon microfiber electrode (CMF) with high electrical conductivity, containing more than 99.00 wt% carbon element (it is composite with polyacrylonitrile), internal resistance of 15-27 mΩ, thickness of 0.2 mm and approximate density of 0.099 g/cm^{-2} was purchased from Redoxkala Company (Iran, Tehran) and catocene liquid with purity of 97.5% containing 23.24-24.4 wt% iron element was purchased from Iran Defence Industries. Electrochemical measurements such as cyclic voltammetry (CV), chrono-potentiometry, galvanostatic charge-discharge (GCD) and electrochemical impedance spectroscopy (EIS) were performed using an EG&G potentiostat model PARSTAT 2273 (Princeton Applied Research Company, US) in 0.1 M sodium sulphate solution and a three-electrode system including Ag/AgCl reference electrode, auxiliary platinum plate electrode with a surface area of 2.0 cm^{-2} and working electrode coated with catocene thin film. EIS studies were performed in the frequency range of 0.1 MHz - 10 kHz at a DC potential of 0.5 V with a sinusoidal potential range of 10 mV. The FT-IR/ATR instrument and elemental analysis by laser-induced breakdown spectroscopy (LIBS) were used to evaluate the surface of the coated film on carbon fibre and to detect the presence of active materials. FT-IR/ATR measurements were performed using a Lumex Infralum-FT08 spectrometer (Russia) equipped with a DTGS detector and MIRacle™ single reflection ATR accessory. The Diamond/ZnSe crystal plate was used. A LIBSCAN100 system manufactured by Photonic Applied Company was also used to record LIBS spectra. This system is equipped with an Nd:YAG laser with a wavelength of 1064 nm, an output energy of 100 mJ, a pulse width of 7±2 nanoseconds and a repetition rate of 1 to 20 Hz. The emitted radiation from the LIBS plasma is collected by optical elements and transferred to the system's

detector, which is capable of recording the spectrum in the range of 182 to 1057 nm with an accuracy of 0.04 nm.

2.2. Preparation of catocene/carbon microfiber electrode

The working electrodes were prepared by coating and preparing a thin film of catocene liquid on the carbon microfiber electrode (Cat/CMF). For this work, first, to remove the surface contamination of the fibre electrode, CMF was washed with acetone solvent and kept at 50°C for one hour; then, the electrode was cooled at room temperature and weighed. Next, concentrations of 0.2 M of the redox reagent were prepared in DMF solvent, and then the electrode with a geometric area of 0.84 cm^2 was placed in the solution for 5.0 minutes. The electrode dipped in the solutions was dried and cooled in the oven for 10.0 minutes to stabilize the catocene thin film on the carbon fibre. The weight of the active materials of the electrode was calculated by calculating the difference in the average weight of the bare and the coated electrode, with a 5-digit analytical balance, model Balance XPR105DR.

2.3. Voltammetry and galvanostatic charge-discharge (GCD) experiments

Cyclic voltammetry (CV) measurements were performed in 0.1 M Na_2SO_4 electrolyte solution with a potential scanning rate of 20.0 – 140.0 mV/s. According to the voltammograms, the specific capacitance can be obtained from the following equation [2]:

$$\boldsymbol{C_{sp}} = \frac{\mathbf{1}}{\mathbf{2}m\nu\Delta V}\int \boldsymbol{i(V)dV} \qquad (1)$$

Where $\boldsymbol{C_{sp}}$ is the specific capacity in Farads per gram (F/g), ν is the potential scan rate (V/s), $\int \boldsymbol{i(V)dV}$ is the area of the cyclic voltammetry curves, and ΔV is the potential window in volts. Galvanostatic charge-discharge (GCD) tests were recorded at different current densities, and specific capacitance was calculated according to equation (2):

$$\boldsymbol{C_{sp}} = \frac{\boldsymbol{I.\Delta t}}{\boldsymbol{Am\Delta V}} \qquad (2)$$

Where I is the discharge current in the unit of ampere (A), Δt is the discharge time duration (s), ΔV is the potential range in the unit of V, and C_{sp} is the specific capacitance (F/g). Also, the specific energy density (E) with the unit of Wh/kg and the specific power density (P) with the unit of W/kg can be calculated with the following relations:

$$\boldsymbol{E} = \frac{\mathbf{1}}{\mathbf{2*3.6}}\boldsymbol{C_{sp}}(\Delta \boldsymbol{V})^{\mathbf{2}} \qquad (3)$$

$$\boldsymbol{P} = \frac{\boldsymbol{E*3600}}{\boldsymbol{\Delta t}} \qquad (4)$$

Where ΔV is the applied potential window, and Δt is the discharge time (seconds).

3. Results and Discussion

3.1. Characterization of the electrode materials

The quality and quantity of catocene thin film formation on the relatively porous carbon microfiber surface were evaluated using scanning electron microscopy (SEM), X-ray energy dispersive spectroscopy (EDS), LIBS, and ATR/FT-IR techniques. Figure 1 shows SEM images and the quality of Fe element distribution on the surface with EDS mapping on the Cat/CMF electrode surface. The distribution of iron atoms in the catocene is relatively low and almost uniform throughout the elemental mapping window. The SEM images reveal the presence of catocene material on the carbon microfibers. The uniform and single-layer distribution on the porous surface of CMF can accelerate electrochemical reaction kinetics and increase the efficiency of redox reactions. Also, in the EDS spectra, the presence of iron element is evident at 6.5 eV compared to the bare electrode. In carbon materials and their composites, very small impurities such as Ca, Mn, Fe, Ni, Zn, Si, S or other elements, depending on their production process, have also been reported [33]. Usually, metallic elements present much more intense peaks than carbon in atomic spectroscopy.

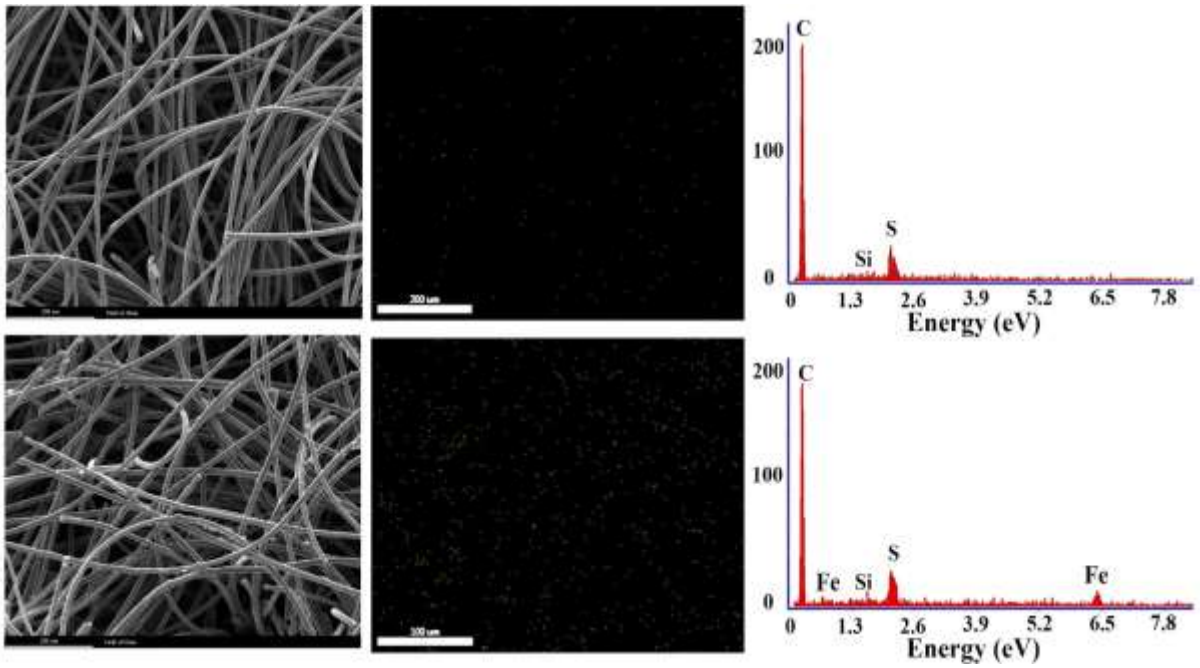

Fig. 1. SEM images, iron element distribution map by EDS method and atomic analysis spectra by EDS for the bare CMF electrode (top) and catocene/CMF electrode (bottom).

LIBS technique is also a powerful method for surface analysis of solids. The LIBS spectra of two electrodes are presented in Fig. 2. For the iron element, about 27 atomic spectral lines have been reported, including 20 atomic emission lines (Fe I) and seven ion emission lines (Fe II), but emission with greater intensity was observed in Fe I 374.55 nm [34]. The analysis of these spectra with NIST LIBS and atomic spectra databases shows that in the CMF electrode, the presence of an iron element is very small, but in the electrode modified with catocene, the presence of an iron element in 374 nm is obvious. In the region near 390 nm, the broad emission peaks appear due to CN atoms or bonds, which can be obtained by the reaction of carbon and nitrogen in air conditions. Atomic emission ranges of carbon elements are reported at 248, 251, 284, 392, 426, 659 and 722 nm. Also, the emission peaks at 600, 575, 567, 520, and 500 nm are related to nitrogen in the surrounding air [35].

FT-IR and ATR spectroscopy are suitable for detecting functional groups of molecules and films coated on electrodes.

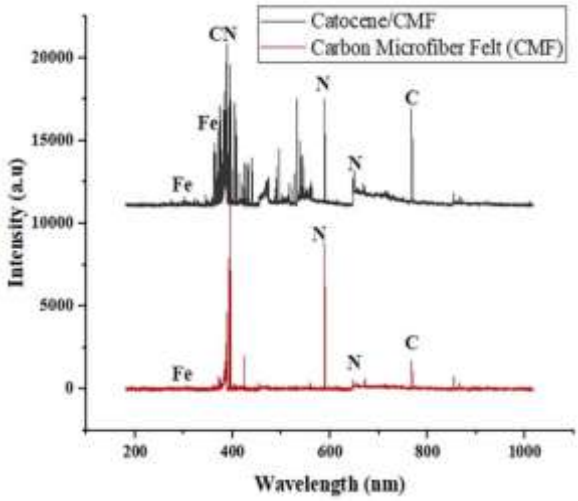

Fig. 2. LIBS elemental analysis of carbon microfiber electrodes (bottom) and microfiber coated with catocene (top).

Figure 3 shows the pure catocene material's FT-IR spectrum and the modified electrode's ATR. The presence of catocene films was not well detected in ATR reflectance spectra, and some weak peaks were observed at a wavenumber near 3000 cm^{-1} due to the low concentration of its thin film on the surface of the electrodes. The FT-IR analysis of catocene, which is similar to ferrocene derivatives, shows ligand characteristics in the wave number range of 2840-3100 cm^{-1} for asymmetric C-H bond stretching

vibrations, 1560-1750 cm^{-1} for C=C stretching vibrations, 1375/1465 cm^{-1} for C-H bending in methylene groups, 905-915 cm^{-1} for C=C bending, and 815 and 1030 cm^{-1} for C-H bending vibrations [20,36].

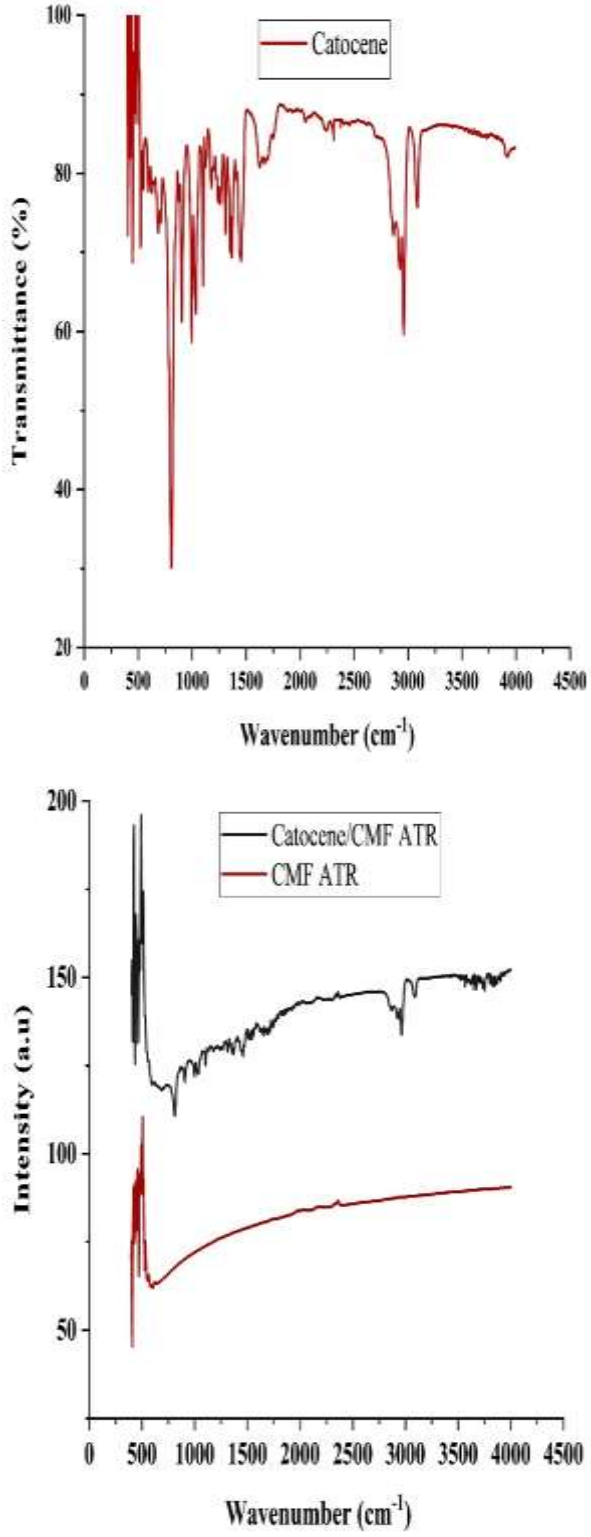

Fig. 3. FT-IR spectra of pure catocene material (top) and ATR of Cat/CMF electrode (bottom)

2.3. Evaluation of the charge storage quality of the modified electrode with CV and EIS techniques

Cyclic voltammetry (CV) tests were conducted on a liquid catocene modified electrode (Cat/CMF) and a bare carbon microfiber electrode (CMF) in a three-electrode system with 1.0 M Na_2SO_4 electrolyte. The potential range was 0.0-0.9 V, and the potential scan rate varied from 20-140 mV/s. In Figure 4-a, the CV curves of the samples at different scan rates are displayed, revealing a peak pair with positive and negative currents associated with oxidation-reduction processes on the Cat/CMF electrode surface. The redox processes of catocene, with the molecular formula $Fe(C_{17}H_{22})$, are similar to those of ferrocene or its derivatives [28,37] and can be oxidized to the $Fe(C_{17}H_{22})^+$ form. The oxidation number of iron in catocene is +2, while its ligand carries a total charge of -2. The reduction of $Fe(C_{17}H_{22})^+$ occurs quasi-reversibly during the reverse potential scan (see Fig. 5). Catocene usually comprises a small amount of four isomeric mixtures with different substitution positions for ethyl groups and diferrocenyl propane compounds. These mixtures are challenging to separate due to their physical and chemical characteristics [38]. It has been suggested that increasing the oxidation potential range of redox substances and expanding the plateau of the voltammetry curve has the potential to enhance the energy storage capacity of cells.

Fig. 6. Proposed reaction for the oxidation-reduction of catocene. By increasing the potential scan rates, the oxidation peaks are shifted to more positive potentials and the reduction peaks are slightly shifted to more negative potentials, as the working electrodes have low ohmic resistance and a shorter time available for electrolyte ions and electrode reactions. In addition, the area under the CV plots and their currents increase as the scan rate increases.

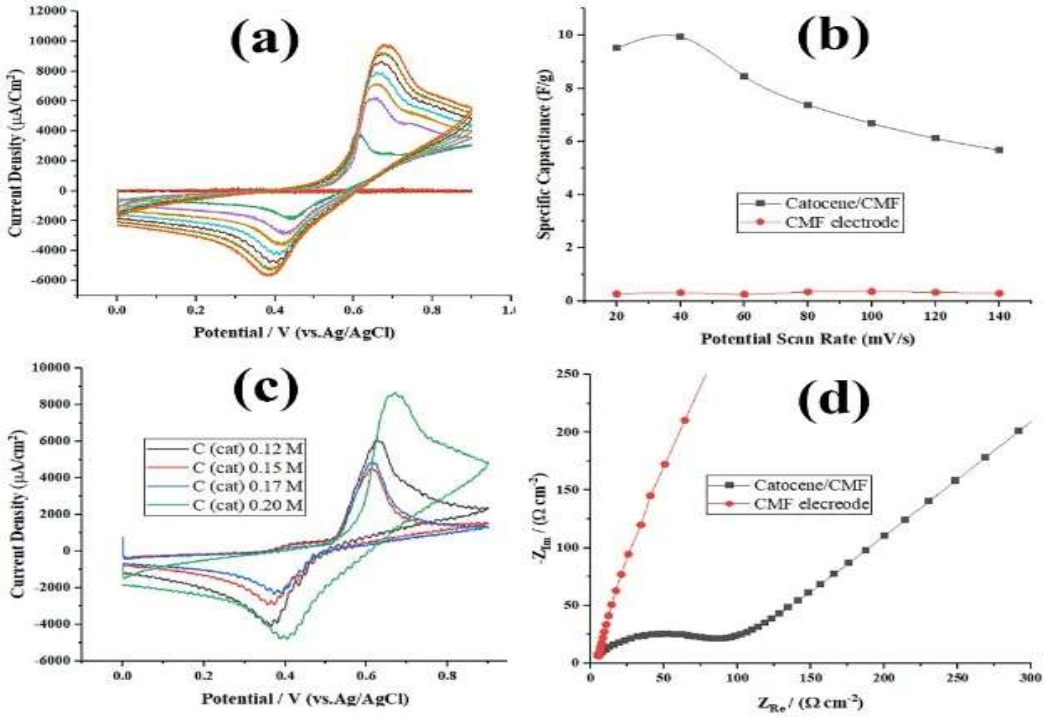

Fig. 4. a) Cyclic voltammetry of self-assembled catocene on carbon microfiber electrode in 1.0 M sodium sulphate solution and different potential scan rates in the range of 20-140 mV/s, b) specific capacitance derived from the voltammograms, c) Voltammetry of self assembled catocene on CMF in its different concentrations in DMF solvent and d) Nyquist diagrams and equivalent circuit of EIS studies by applying DC potential close to 0.5 V and AC potential of 10.0 mV in the frequency range of 0.10 Hz to 0.100 kHz.

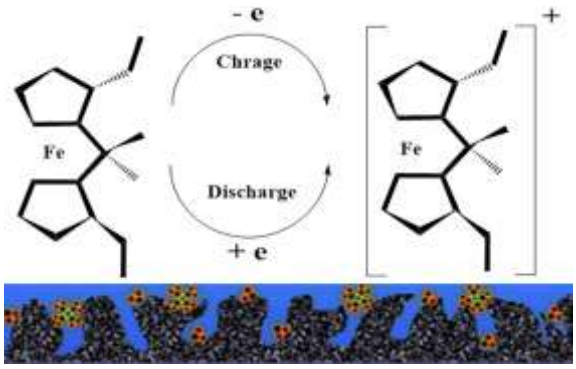

Fig. 5. Proposed reaction for the oxidation-reduction of catocene.

The anodic peak of the cathode has a linear relationship with the square root of the potential scan rate according to the following equation: I (mA) = 19.91 × $\upsilon^{1/2}$ (V s^{-1}) + 2.26 (R^2 = 0.9993): this indicates that the Faraday reaction is diffusion controlled [39]. Because cyclic voltammograms show intense, clearly separated oxidative and reductive peaks, and the peak current response is proportional to the square root of the scan rate (I ~ $\nu^{1/2}$), this thin-film electrode should be classified as a battery-type electrode [40,41]. At the potential scan rate of 20.0 mV/s, the slope of the Tafel equation (Log (I /A)-E (V)), which is equal to n(1-α)F/2.3 RT, was calculated to be 10.52 decade/V. Therefore, the value of the cathodic transfer coefficient is equal to α=0.48 (in n=1). The value of α for catocene is close to 0.5, indicating the symmetry of the voltammograms and the lower activation energy barrier for the formation of the active and intermediate complexes in the electrochemical reaction. Fig. 4-b also shows that the specific capacity of the Cat/CMF electrode is significantly higher than that of the bare electrode. As the concentration of catocene in the DMF solvent increases, the anodic-cathode current of the modified electrode increases, as shown in Fig. 4-c, indicating the increase in surface coverage and self-accumulation of catocene on the CMF electrode. Here, the surface coverage of catocene (Γ) on the

carbon microfiber electrode was calculated according to Eq. (5) [42]:

$$\Gamma = \frac{Q}{nFA} \quad (5)$$

Where Q is the area below the oxidation peak in CV curves of the modified electrode, n is the number of electrons participating in the reaction (n=1), A is the electrode surface area, and F is Faraday's constant. The surface coverage's Γ for the modified electrode at different scan rates is presented in Table 1. It can be observed that the value of Γ has decreased with the increase in scan rate because, at higher rates, there is less time for the reaction of redox material. On the other hand, because the amount of electric charge changes with the scan rate, the electrochemical behaviour of the electrode is battery-like [41].

Table 1. The effect of potential scan rate on the amount of catocene surface coverage on the carbon microfiber electrode.

Scan rate, ν [mV s^{-1}]	Q, mC	Electrochemical rugosity, Γ [× 10^6 mol cm^{-2}]
20.0	18.83	8.13
40.0	19.66	8.49
60.0	16.74	7.23
80.0	14.61	6.31
100.0	13.27	5.73
120.0	12.11	5.23
140.0	11.24	2.85

In EIS studies at a DC potential of +0.5 V, Nyquist diagrams presented in Fig. 4-d. The curved semicircle at high frequencies is related to the charge transfer resistance of the redox material and the electrical double-layer capacity. The appropriate equivalent circuit for the semi-circular part of the Nyquist diagrams, similar to the Randles circuit, includes the ohmic resistance of the solution (R_s), the catocene oxidation charge transfer resistance (R_{ct}), the constant phase element of the electric double layer capacitance (CPE_{dl}), and Warburg element (W) related to the semi-infinite diffusion process. The impedance of CPE and W can be expressed as [42]:

$$Z_{CPE} = (Y_0 j\omega)^{-n} \quad (6)$$

$$Z_W = Y_0^{-1}(j\omega)^{-1/2} \quad (7)$$

where Y_0 (the admittance parameter, S cm^{-2} s^{-n}) and n (dimensionless exponent) are two parameters independent of frequency; $j = (-1)^{1/2}$, and ω is angular frequency = 2πf.

The microscopic roughness of the CMF electrode causes an inhomogeneous distribution in the solution resistance and the double-layer capacitance. This issue leads to appearance of depressed semicircles or constant phase elements in the Nyquist plots. Also, the diffusion-controlled process at low frequencies leads to the appearance of the Warburg element in the Cat/CMF redox process.

Table 2 shows the values of the equivalent circuit elements calculated by fitting the experimental results. The goodness of the fit can be judged by the estimated relative errors presented in the parentheses. According to the values of the electrical equivalent elements reported in this Table, the charge transfer resistance (R_{ct}) for oxidation of self-assembled catocene on the CMF electrode is 140.2 (±3.7%) Ω.cm^{-2}, compared to 3251.9 (±3.2%) Ω.cm^{-2} for bare CMF electrode. The apparent electron transfer rate (k_{app}) has an inverse relationship with the charge transfer resistance on Nyquist diagrams. In other words, as R_{ct} increases, the rate of electrode reactions decreases [39]. Therefore, the reaction rate of Cat/CMF at a DC potential of +0.5 V is close to 23 times higher than that of the CMF electrode.

3.3. Galvanostatic charge-discharge studies

In this section, the galvanostatic charge-discharge (GCD) curves of the samples were evaluated at different current densities in the potential window range of 0.0 - 0.9 V. From Fig. 6-a, it can be seen that the capacitive behaviour of the carbon microfiber electrode in aqueous sodium sulphate electrolyte is similar to that of the electrochemical double layer capacitors (EDLCs) and the Cat/CMF electrode has a battery-like behaviour. In EDLC capacitors, the charge-discharge behaviour is

triangular due to the lack of transfer resistance in redox reactions.

Table 2. The values of the elements in equivalent circuit and the corresponding relative errors for the oxidation of self-assembled catocene on the CMF electrode.

Electrode	R_s (Ω cm^2)	R_{ct} (Ω cm^2)	*CPE*		$W \times 10^4$ (Ω cm^2)
			$Y_0 \times 10^{-6}$	*n*	
Bare CMF	8.90	3251.9 (±3.2%)	0.08337 (1.9%)	0.3250 (3.13%)	-
Cat/CMF	9.10	140.2 (±3.7%)	0.09132 (3.1%)	0.3460 (2.4%)	0.2873 (2.3%)

The correlation of the specific capacitance (F/g) of the electrodes from their discharge curves at different current densities is calculated according to equation (2) and shown in Fig. 6 (c and d). Here, the discharge time of the samples increases as the current density decreases. The specific capacity of the Cat/CMF electrode at a current density of 0.55 A/g is equal to 39.76 F/g. At constant electrode surface area, the capacitance of the Cat/CMF electrode is equal to 180 mF/cm^2; for the CMF electrode with EDLC behaviour, it is approximately 0.91 mF/cm^2. Also, the specific capacitance of this catocene-based capacitor decreases with increasing current density, probably due to the limitation of mass transfer and the diffusion mechanism of redox substances. On the other hand, an instantaneous voltage drop, known as the IR drop, occurs when the SC switches from charging to discharging due to the system's combined ohmic resistance, electrolyte and contact resistances. A lower IR drop value indicates the low ohmic nature of the electrode/electrolyte. The galvanostatic discharge curves in Figure 6 (a-b) show an IR drop close to 0.5 V. It is also clear from the EIS studies presented in Table 2, that the CMF electrode and sodium sulphate electrolyte have an equivalent series resistance close to 8.9 Ω cm^2. This results in a drop in the effective potential of the capacitor.

Energy density versus power density diagram (Ragone plot) and cyclic stability tests of the modified electrode was performed at a current density of 0.83 A/g for 3000 charge-discharge cycles, as presented in Fig. 7. At the current density of 0.83 A/g, the supercapacitor behaviour of catocene has an energy density of 2.5 Wh/kg and a power density of 373.8 W/kg. Also, with the increase in power densities, energy density values have a downward trend. The overall capacity of the capacitors in successive charge-discharges, up to 3000 cycles, shows that the capacity of the Cat/BPPG electrode decreases by approximately 30%.

The electrochemical efficiency of a number of similar electrodes is compared in Table 3. It is observed that the self-assembled catocene redox on the carbon microfiber electrode has a high power density despite its relatively low energy density. In other words, its discharge kinetics is significantly high. By using MWCNTs chemically functionalized with ferrocene, the specific capacitance at a current density of 0.25 A/g has been reported to be approximately 50 F/g [20]. Considering that the production steps and functionalization cost of the mentioned electrodes are high, as well as a limited amount of redox substances sticking on the surface in these conditions, it seems that the use of liquid catocene is also a suitable solution to improve the efficiency of electrochemical supercapacitors.

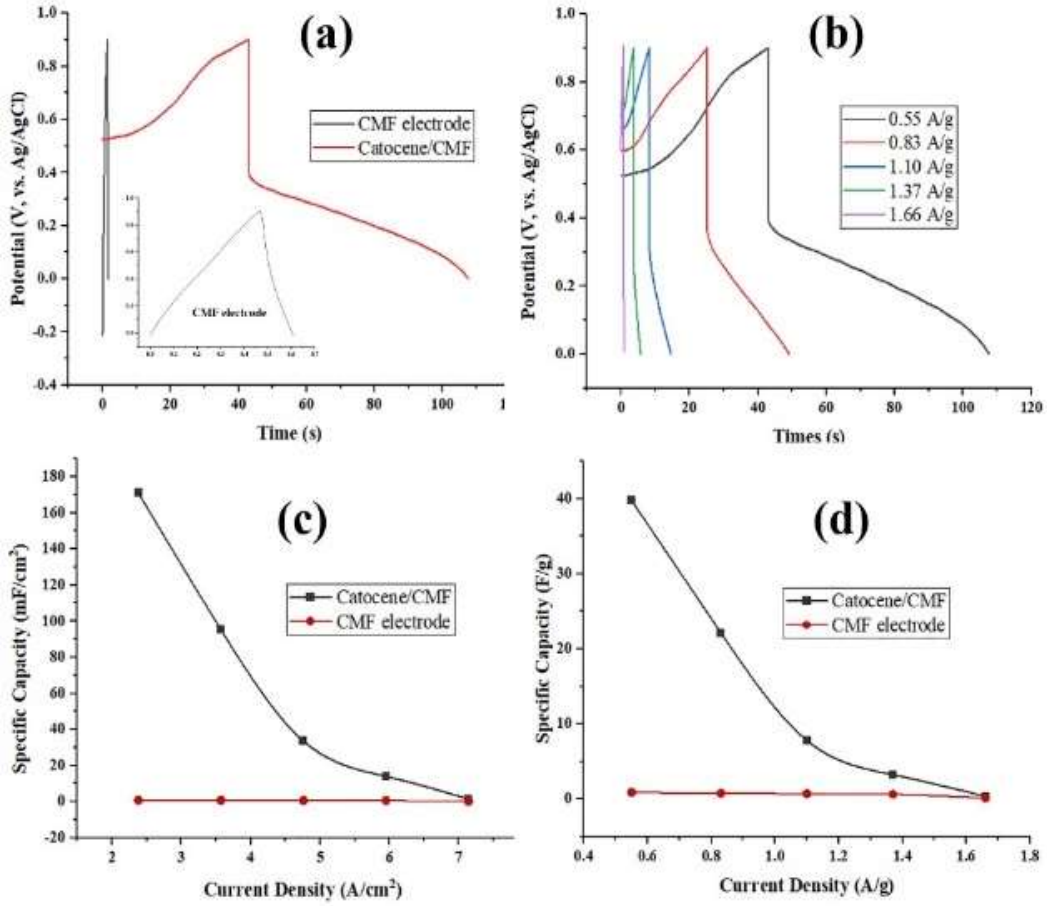

Fig 6. a) Comparison of galvanostatic charge-discharge (GCD) curves of Cat/CMF electrode and uncoated carbon microfiber, b) GCD curves of electrodes at different current densities, c) specific capacity (F/g) in various current densities per 1.0 cm^2 electrode surface area and d) specific capacity of the electrodes per unit of electrode surface area ((F/cm^2).

Table 3. The supercapacitor performance of some carbon-felt-modified electrodes is in the literature.

Electrode material	Electrolyte	Current density (A/g)	specific capacity (F/g)	energy density (Wh/kg)	Power density (W/kg)	Cycles	Stability (%)	Ref.
V_2O_5 /CF [(a)]	5.0 M LiCl		492	-	-	2000	89.7	[15]
Ag-doped MnO_2/CC [(b)]	1.0 M Na_2SO_4	0.5	520.8	-	-	2000	90.6	[43]
MnO_2/CF [(c)]	2.0 M Li_2SO_4	0.2	187.5	-	-	10000	99.0	[16]
$NiFe_2O_4$/CF [(d)]	3.0 M KOH	1.0	490	39	410	5000	94.2	[17]
$CoSe_2$/CF [(e)]	6.0 M KOH	1.0	621	22.4	823.1	100000	84.7	[19]
h-BN/C [(f)]	2.0 M KOH	0.5	250	17	245	1000	-	[44]
Fc-MWCNTs [(g)]	2.0 M KOH	0.25	50	-	-	5000	90.8	[20]
Cat/CMF [(h)]	0.1 M Na_2SO_4	0.83	39.8 (at 0.55 A/g)	2.5	373.8	3000	70.0	This work

(a) V_2O_5 nanosheets assembled on carbon fiber felt (V_2O_5 /CF)
(b) Ag-Doped Urchin-like MnO_2 on Carbon Cloth (Ag-doped MnO_2/CC)
(c) Binder-Free Electro-Deposited MnO_2 @3D Carbon Felt Network (MNO_2/CF)
(d) Nickel ferrite coated on carbon felt ($NiFe_2O_4$/CF)
(e) Hydrothermal deposited urchin-like $NiCo_2O_4$ on carbon felt ($NiCo_2O_4$/CF)
(f) $CoSe_2$/carbon fiber felt electrode ($CoSe_2$/CF)
(g) Ferrocene functionalized multi-walled carbon nanotubes (Fc-MWCNTs)
(h) Carbon-modified hexagonal boron nitride nanosheet (*h*-BN/C) nanocomposite (*h*-BN/C)

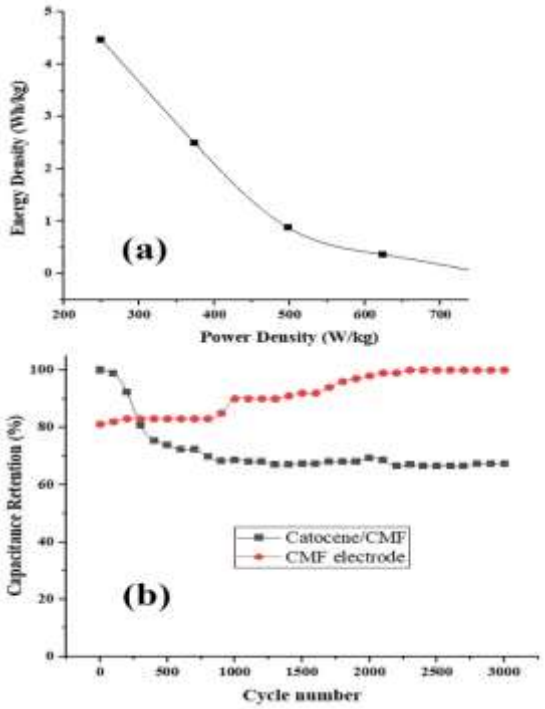

Fig. 7. Ragone plots of supercapacitive behaviours of Cat/CMF and b) cyclic stability in current density of 0.83 A/g

4. Conclusion

In summary, the voltammetry and supercapacitor behaviour of a liquid redox, catocene, in a self-assembled form on the carbon microfiber electrode was investigated. Spectroscopic studies showed that the liquid catocene had a relatively more uniform distribution and a favourable interaction with the carbon microfiber surface. The oxidation of the catocene on the CMF is diffusion-controlled with battery-like behaviour and shows a typical specific capacity of 39.76 F/g at a current density of 0.55 A/g. Based on the geometric surface area of the electrode, the capacitance of the Cat/CMF electrode is 180 mF/cm^2 compared to 0.91 mF/cm2 for the bare CMF. At a current density of 0.83 A/g, the supercapacitor has an energy density of 2.5 Wh/kg and a power density of 373.8 W/kg. As the power densities increase, the energy densities also tend to decrease. After almost 3000 consecutive charge-discharge cycles, the total capacity decreases by about 30%. Considering the relatively difficult production steps and costs of chemically functionalized carbon electrodes, the use of liquid redox materials such as catocene seems to be a suitable case for improving the efficiency of electrochemical supercapacitors.

Acknowledgements

The authors are grateful for the financial support of this work by Malek-ashtar University of Technology (I.R. Iran).

Conflicts of Interest

The author declares that there is no conflict of interest regarding the publication of this manuscript. In addition, the authors have entirely observed the ethical issues, including plagiarism, informed consent, misconduct, data fabrication and/or falsification, double publication and/or submission, and redundancy.

References

[1] Wang, Y., Zhang, L., Hou, H., Xu, W., Duan, G., He, S., Liu, K., & Jiang, S. (2020). Recent progress in carbon-based materials for supercapacitor electrodes: a review. *Journal of Materials Science, 56*(1), 173–200.

[2] Sharma, S., & Chand, P. (2023). Supercapacitor and electrochemical techniques: A brief review. *Results in Chemistry*, *5*, 100885.

[3] Shah, S. S., Aziz, M. A., Mahfoz, W., & Akhtaruzzaman, M. (2023). Types of Supercapacitors. In *Biomass-Based Supercapacitors: Design, Fabrication and Sustainability* (pp. 93–104). John Wiley & Sons, Ltd.

[4] Shaikh, N. S., Ubale, S. B., Mane, V. J., Shaikh, J. S., Lokhande, V. C., Praserthdam, S., Lokhande, C. D., & Kanjanaboos, P. (2022). Novel electrodes for supercapacitor: Conducting polymers, metal oxides, chalcogenides, carbides, nitrides, MXenes, and

their composites with graphene. *Journal of Alloys and Compounds*, *893*, 161998.

[5] Han, Y., & Dai, L. (2019). Conducting Polymers for Flexible Supercapacitors. *Macromolecular Chemistry and Physics*, *220*(3), 1800355.

[6] Ma, Y., Xie, X., Yang, W., Yu, Z., Sun, X., Zhang, Y., Yang, X., Kimura, H., Hou, C., Guo, Z., & Du, W. (2021). Recent advances in transition metal oxides with different dimensions as electrodes for high-performance supercapacitors. *Advanced Composites and Hybrid Materials*, *4*(4), 906–924.

[7] Liang, R., Du, Y., Xiao, P., Cheng, J., Yuan, S., Chen, Y., Yuan, J., & Chen, J. (2021). Transition Metal Oxide Electrode Materials for Supercapacitors: A Review of Recent Developments. *Nanomaterials 11*(5), 1248.

[8] Yan, J., Liu, T., Liu, X., Yan, Y., & Huang, Y. (2022). Metal-organic framework-based materials for flexible supercapacitor application. *Coordination Chemistry Reviews*, *452*, 214300.

[9] Ansari-asl, Z., Neisi, Z., Sedaghat, T., & Nobakht, V. (2019). Synthesis, characterization, and electrochemical properties of polyaniline/Co(II) metal-organic framework composites. *Applied Chemistry Today*, *14*(51), 251–266.

[10] Lakra, R., Kumar, R., Sahoo, P. K., Thatoi, D., & Soam, A. (2021). A mini-review: Graphene based composites for supercapacitor application. *Inorganic Chemistry Communications*, *133*, 108929.

[11] Wu, Q. S., Bigdeli, F., Rouhani, F., Gao, X. M., Kaviani, H., Li, H. J., Wang, W., Liu, K. G., Hu, M. L., Cai, X. Q., & Morsali, A. (2021). New 3D Porous Silver Nanopolycluster as a Highly Effective Supercapacitor Electrode: Synthesis and Study of the Optical and Electrochemical Properties. *Inorganic Chemistry*, *60*(3), 1523–1532.

[12] Damiri, S., Varzaneh, H. Y., & Ebrahimi, H. R. (2011). PEG-assisted electrochemical growth of lead oxide nanodendrites with strongly enhanced charge storage capacity. *Materials Letters*, *65*(17–18), 2598–2600.

[13] Yu, M., & Feng, X. (2019). Thin-Film Electrode-Based Supercapacitors. *Joule*, *3*(2), 338–360.

[14] Oje, A. I., Ogwu, A. A., Mirzaeian, M., Oje, A. M., & Tsendzughul, N. (2019). Silver thin film electrodes for supercapacitor application. *Applied Surface Science*, *488*, 142–150.

[15] You, M., Zhang, W., Yan, X., Jiang, H., Miao, J., Li, Y., Zhou, W., Zhu, Y., & Cheng, X. (2021). V2O5 nanosheets assembled on 3D carbon fiber felt as a free-standing electrode for flexible asymmetric supercapacitor with remarkable energy density. *Ceramics International*, *47*(3), 3337–3345.

[16] Prabu, V., Geetha, K., Sekar, R., & Ulaganathan, M. (2023). Binder-Free Electro-Deposited MnO2 @3D Carbon Felt Network: A Positive Electrode for 2V Aqueous Supercapacitor. *Energy Technology*, *11*(2), 2201345.

[17] Azizi, S., Askari, M. B., Rozati, S. M., & Masoumnezhad, M. (2024). Nickel ferrite coated on carbon felt for asymmetric supercapacitor. *Chemical Physics Impact*, *8*, 100543.

[18] Achour, W., Ynineb, F., Hadjersi, T.,

Moulai, F., Ifires, M., Khen, A., Manseri, A., & Kechouane, M. (2023). Hydrothermal deposition of urchin-like $NiCo_2O_4$ on carbon felt as performed flexible electrodes for supercapacitors. *Journal of Applied Electrochemistry*, *53*(7), 1405–1419.

[19] Du, L., Zhang, R., Zhou, J., Li, J., Huang, X., & Luo, J. (2022). Microwave-synthesized self-supporting $CoSe_2$/carbon fiber felt electrode for ultra–high cycling life flexible supercapacitors. *International Journal of Hydrogen Energy*, *47*(26), 12855–12864.

[20] Ali, G. A. M., Megiel, E., Cieciórski, P., Thalji, M. R., Romański, J., Algarni, H., & Chong, K. F. (2020). Ferrocene functionalized multi-walled carbon nanotubes as supercapacitor electrodes. *Journal of Molecular Liquids*, *318*, 114064.

[21] Hu, M. L., Abbasi-Azad, M., Habibi, B., Rouhani, F., Moghanni-Bavil-Olyaei, H., Liu, K. G., & Morsali, A. (2020). Electrochemical Applications of Ferrocene-Based Coordination Polymers. *ChemPlusChem*, *85*(11), 2397–2418.

[22] Teimuri-Mofrad, R., Hadi, R., & Abbasi, H. (2019). Synthesis and characterization of ferrocene-functionalized reduced graphene oxide nanocomposite as a supercapacitor electrode material. *Journal of Organometallic Chemistry*, *880*, 355–362.

[23] Khordadpour Siahkal Mahalleh, M., Ahour, F., & Keshipour, S. (2023). Development of copper electrochemical sensor using D-penicillamine functionalized graphene oxide modified electrode. *Applied Chemistry Today*, *18*(67), 71–90.

[24] Arvand, M., Pourhabib, A., & Mousavi, S. J. (2023). Electrochemical exfoliated graphene oxide nanosheets modified graphite electrode for clozapine sensing. *Applied Chemistry Today*, *18*(69), 57–68.

[25] Habibi Shabestary, B., & Golbon Haghighi, M. (2023). Synthesis, Characterization and DNA binding studies of Platinum Complexes with Imine Ferrocene Ligand. *Applied Chemistry Today*, *18*(66), 225–240.

[26] Nemati, F., Farrokhi, H., & Jazirehpour, M. (2017). Chemical synthesis and characterization of polypyrrole with novel morphology prepared via self-reactive MnO_2 microcube as sacriï• cial template and oxidizing agent. *Applied Chemistry Today*, *12*(45), 65–70.

[27] Saha, P., Yadav, V. K., Gurunarayanan, V., Ramapanicker, R., Singh, J. K., & Gopakumar, T. G. (2020). Revealing the Limits of Intermolecular Interactions: Molecular Rings of Ferrocene Derivatives on Graphite Surface. *Journal of Physical Chemistry Letters*, *11*(1), 297–302.

[28] Kurapati, N., Pathirathna, P., Ziegler, C. J., & Amemiya, S. (2019). Adsorption and Electron-Transfer Mechanisms of Ferrocene Carboxylates and Sulfonates at Highly Oriented Pyrolytic Graphite. *ChemElectroChem*, *6*(22), 5651–5660.

[29] Damiri, S., Pouretedal, H. R., & Mahmoudi, M. (2022). Sensitive Electrocatalytic Assay of Cyclotetramethylene Tetranitramine (HMX) Explosive on Carbon Nanotube/Ag Nanocomposite Electrode. *Iranian Journal of Catalysis*, *12*(1), 69–76.

[30] Sa'at, M., Yarmohammadi, M., Zamani

Pedram, M., Shahidzadeh, M., & Amini-Fazl, M. S. (2019). Evaluation of the catocene/graphene oxide nanocomposite catalytic activity on ammonium perchlorate thermal decomposition. *International Journal of Chemical Kinetics*, *51*(5), 337–345.

[31] Feng, H., Suo, Q., Zhang, C., Liu, X., & Ma, X. (2021). Component Analysis of Industrial Grade Catocene and Preparation of Binuclear Ferrocene. *Acta Armamentarii*, *42*(5), 961.

[32] Xiaoju, L., Qi, S., Haitao, F., Chi, Z., Xiaoyan, M., Xiaoju, L., Qi, S., Haitao, F., Chi, Z., & Xiaoyan, M. (2021). Theoretical and experimental study on synthesis of high-content catocene. *Journal of Beijing University of Aeronautics and Astronautics*, *47*(12), 2514–2520.

[33] Saxena, K., Kumar, P., & Jain, V. K. (2011). Synthesis of carbon microfibers by chemical vapor deposition during the catalytic decomposition of turpentine oil. *New Carbon Materials*, *26*(5), 356–360.

[34] Idris, N., Lahna, K., Fadhli, & Ramli, M. (2017). Study on Emission Spectral Lines of Iron, Fe in Laser-Induced Breakdown Spectroscopy (LIBS) on Soil Samples. *Journal of Physics: Conference Series*, *846*(1).

[35] Ralchenko, Y., & Kramida, A. (2020). Development of NIST Atomic Databases and Online Tools. *Atoms*, *8*(3), 56.

[36] Paul, A., Muthukumar, S., & Prasad, S. (2020). Application of Room Temperature Ionic Liquid As Sensing Modality for Selective Detection of Important Phenylpyperidine Analogue. *ECS Meeting Abstracts*, *MA2020-01*(35), 2451–2451.

[37] Chemistry, N. T.-J. of S., & 2007, undefined. (2007). Cyclic voltammetric studies of ferrocene in nonaqueous solvents in the temperature range from 248.15 to 298.15 K. *SpringerNG TsierkezosJournal of Solution Chemistry*, *36*(3), 289–302.

[38] Xiaoju, L., Qi, S., Haitao, F., Chi, Z., Xiaoyan, M., Xiaoju, L., Qi, S., Haitao, F., Chi, Z., & Xiaoyan, M. (2021). Theoretical and experimental study on synthesis of high-content catocene. *Journal of Beijing University of Aeronautics and Astronautics*, *47*(12), 2514–2520.

[39] Faulkner, A. J. B. L. R. (2008). Electrochemical Methods: Fundamentals and Applications, 2nd Edition. In *Wiley*.

[40] Noori, A., El-Kady, M. F., Rahmanifar, M. S., Kaner, R. B., & Mousavi, M. F. (2019). Towards establishing standard performance metrics for batteries, supercapacitors and beyond. *Chemical Society Reviews*, *48*(5), 1272–1341.

[41] Gogotsi, Y., & Penner, R. M. (2018). Energy Storage in Nanomaterials - Capacitive, Pseudocapacitive, or Battery-like? *ACS Nano*, *12*(3), 2081–2083.

[42] Damiri, S., Pouretedal, H. R., & Heidari, A. (2016). Fabrication of a nanostructured TiO_2/carbon nanotube composite electrode for voltammetric and impedimetric determination of NTO explosive in the water and soil samples. *International Journal of Environmental Analytical Chemistry*, *96*(11), 1059–1073.

[43] Feng, Y., Qu, H., Wang, Y., Wang, L., Wang, Y., Yang, D., Ding, B., Sun, Y., Guo, J., & Dai, S. (2024). Facile Synthesis of Ag-Doped Urchin-like MnO_2 on Carbon Cloth for

Supercapacitors. *Materials*, *17*(6), 1312.

[44] Li, T., Jiao, X., You, T., Dai, F., Zhang, P., Yu, F., Hu, L., Ding, L., Zhang, L., Wen, Z., & Wu, Y. (2019). Hexagonal boron nitride nanosheet/carbon nanocomposite as a high-performance cathode material towards aqueous asymmetric supercapacitors. *Ceramics International*, *45*(4), 4283–4289.